Technical Note

False-Positive Analysis of Functional MRI During Simulated Deep Brain Stimulation: A Phantom Study

Ho-Ling Liu, PhD,[1,2] Hsin-Mei Chen, BS,[1] Yu-Chien Wu, MD, PhD,[3,6] Siew-Na Lim, MD,[4] Chih-Mao Huang, MS,[1,5] Yuan-Yu Hsu, MD,[5] Yau-Yau Wai, MD,[2] and Tony Wu, MD, PhD[4]*

Purpose: To investigate the false-positive activations/deactivations in functional MRI (fMRI) of deep brain stimulation (DBS) using a phantom.

Materials and Methods: fMRI experiments were performed on a 1.5T scanner using a single-shot gradient-echo echo-planar imaging (GE-EPI) sequence (TR/TE/FA = 6000 msec/60 msec/90°) on an agar-gel phantom inserted with DBS electrodes. During the experimental blocks, two-second stimuli were delivered during the interscan waiting time (ISWT), which was adjusted by changing the number of slices acquired within the TR (3500 msec with 30 slices and 5160 msec with 10 slices). Data were analyzed using SPM2 software, and the false-positive voxels were detected with five different P-value thresholds.

Results: The number of false-positive voxels in experimental conditions had no significant differences from those in control conditions with either long or short ISWT, which increased with the P-value threshold from zero at $P < 0.0001$ to approximately 40 at $P < 0.05$. The pattern of increasing number of false-positive reactions along with P-value was similar between all conditions.

Conclusion: False-positive findings from fMRI with similar experimental design can be well controlled with a statistical threshold of $P < 0.001$ or tighter. The short ISWT of 3500 msec did not increase false-positive reactions compared to the long ISWT of 5160 msec.

Key Words: functional MRI; deep brain stimulation; interscan waiting time; EPI; false-positive reaction
J. Magn. Reson. Imaging 2008;27:1439–1442.

DEEP BRAIN STIMULATION (DBS) is an established technique that involves minimal brain invasion to stimulate deep brain nuclei, including the middle or subthalamic nucleus and general basal ganglia. This technique is effective, and has been widely used on patients with Parkinson diseases (PD) (1). Some other neurological disorders may also benefit from DBS, such as movement disorders, chronic pain, and epilepsy (2). Unlike surgical approaches, DBS is reversible, and also unlike systematic pharmaceutical approaches, DBS targets pathological sites more directly.

Although with known therapeutic benefits, the underlying mechanism of DBS is still not clear. By adjusting the stimulation frequency, DBS may serve as an inhibition or stimulator to neuronal activity. Therefore, functional MRI (fMRI) may be an effective method to study the neurophysiology reactions caused by DBS. fMRI offers several advantages: it is noninvasive, has superior spatial/temporal resolution, and is widely available. Recently, researchers have found that during DBS, patients experienced emotional changes (3,4). Using DBS may become another treatment option for psychiatric disorders such as depression, mood disorders, and bipolar disorder, and fMRI may be suitable to monitor treatment results.

The safety and feasibility of fMRI acquisitions interleaved with DBS have been studied on a NaCl solution-filled phantom by Georgi et al (5) and on PD patients by Jech et al (6), respectively. In addition, research showed that neuronal activations in the neighborhood of the electrodes as well as cortical and subcortical areas were

[1]Department of Medical Imaging and Radiological Sciences, Chang Gung University, Taoyuan, Taiwan.
[2]MRI Center, Chang Gung Memorial Hospital, Taoyuan, Taiwan.
[3]Department of Radiology, University of Wisconsin-Madison, Madison, Wisconsin, USA.
[4]The Waisman Laboratory for Brain Imaging and Behavior, University of Wisconsin-Madison, Madison, Wisconsin, USA.
[5]Epilepsy Section, Department of Neurology, Chang Gung Memorial Hospital, Taoyuan, Taiwan.
[6]Department of Medical Imaging, Buddhist Tzu Chi General Hospital–Taipei, Taipei, Taiwan.
Contract grant sponsor: National Science Council of Taiwan; Contract grant number: NSC94-2314-B-182-006; Contract grant sponsor: Chang Gung Memorial Hospital; Contract grant number: CMRPD140052.
*Address reprint requests to: T.W., Epilepsy Section, Department of Neurology, Chang Gung Memorial Hospital, Taoyuan, Taiwan, 5 Fuhsing Street, Kweishan, Taoyuan 333, Taiwan.
E-mail: tonywu@adm.cgmh.org.tw
Received January 23, 2007; Accepted September 7, 2007.
DOI 10.1002/jmri.21222
Published online in Wiley InterScience (www.interscience.wiley.com).

detected by fMRI during DBS with electrodes located at thalamic and subthalamic nuclei (3,6,7). In epilepsy patients, our previous study found that high-frequency DBS to anterior thalamic nuclei (ATN) induced blood oxygenation-level dependent (BOLD) signal decreases in several brain regions (8). However, the validation of fMRI signals associated with DBS is not well documented, especially the differentiability between real activations/deactivations and task-correlated signal changes that could potentially result from additional noises from the DBS apparatus. False-positive activations may cause improper interpretation of the mechanism of DBS, and hence may be obstacles to the future application of DBS.

This study aimed to investigate possible false-positive activations in fMRI experiments during DBS. Two different interscan waiting times (ISWT), defined as the time interval between the end of the EPI acquisition window in a TR and the radio frequency (RF) excitation pulse of the subsequent TR, were included in the experiment. Because the stimulator was turned on within the ISWT, too short an ISWT may cause BOLD signal variations in the following measurement if the electric currents generated by DBS would have a long decay constant. An agar-gel phantom was scanned to simulate fMRI during DBS and the resulting false-positive rates obtained at different statistical thresholds (*P*-values) were compared between the two experimental conditions and their corresponding control conditions.

MATERIALS AND METHODS

The study was performed on an agar-gel phantom ($\sim 11 \times 17 \times 5$ cm^3) on a 1.5T Philips Gyroscan Intera MRI scanner. The phantom contained 9.0% agarose and 0.07% sodium (wt/wt), which led to a conductivity around 0.33 S/m (9,10). The estimated conductivity was in the range of the published data for human brain tissues (0.15 S/m for white matter and 0.45 S/m for gray matter) (11,12). DBS electrodes (Medtronic 3387; Medtronic, Minneapolis, MN, USA) were inserted into the phantom and the tip was positioned near the center of the phantom. During the experiments, the stimulator (Medtronic 7428; Medtronic) was kept outside the scanner room and was connected to the leads via the twist-lock screening cable (7-m long). The electrodes were activated by manually connecting the leads to the neurostimulator, using a cable plug. The stimulation parameters, which were reported in the literature for DBS studies in patients with epilepsy, were amplitude = 5.0 V, pulse width = 90 μsec, and frequency = 145 Hz (13).

Data Acquisition

We designed two stimulation conditions. The experimental condition consisted of interleaved five stimulation-off and four stimulation-on blocks, while the control condition consisted of nine blocks of stimulation-off. The duration of each block was 42 seconds with seven imaging repetitions. During the stimulation-on blocks, each stimulus was started immediately after each EPI readout, and lasted for approximately two seconds. To evaluate whether BOLD signals were affected by the decay of electric current after the neurostimulator was switched off, we studied two time intervals between the end of stimulation and the subsequent RF excitation, which was achieved by varying the ISWT. ISWT was varied by changing the number of slices acquired per TR, which was set to be 6000 msec across all experiments in this study. The timing paradigms of EPI acquisition, DBS block, and the ISWT are described in Fig. 1. When 30 slices were acquired, the ISWT was 3500 msec and was denoted as short ISWT. For 10 slices, the ISWT was 5160 msec and was denoted as long ISWT.

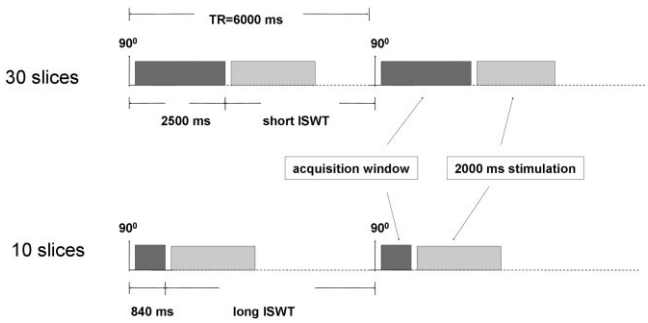

Figure 1. The time sequence of the fMRI acquisition and the DBS. TR was set to be 6000 msec, and the duration of DBS was set to be 2000 msec across the whole experiment. When 30 slices per TR were acquired, there would be a short ISWT of 3500 msec between the end of the acquisition window and the subsequent 90° RF excitation. On the other hand, when 10 slices were acquired, there would be a long ISWT of 5160 msec.

A single-shot gradient-echo EPI (GE-EPI) sequence was applied for the fMRI scans. The imaging parameters were TR/TE/θ = 6000 msec/60 msec/90°, field of view (FOV) = 192 mm, matrix size = 64 × 64, slice thickness = 3 mm, and dynamic volumes =63. T1-weighted images were obtained by using a conventional spin-echo sequence (TR/TE = 400 msec/12 msec, FOV = 256 mm, matrix size = 256 × 256), with the same slice thickness and locations as the functional scans.

Data Analysis

fMRI data were analyzed using Statistical Parametric Mapping software (SPM2; Wellcome Department of Neurology, London, UK). Spatial smoothing was performed with a Gaussian kernel of 5 mm full-width-at-half-maximum (FWHM). After preprocessing, the t-map of the central slice, i.e., the 15th for 30 slices and the fifth for 10 slices, was selected for further computation. The agar-gel phantom should not have neuronal activity regardless stimulation conditions or lengths of ISWT. Thus, any significant activation/deactivation detected was considered as false-positive activation/deactivation. To explore the relation of false-positive reactions to the *P*-value threshold, voxels with t-value exceeding five *P*-value thresholds, 0.05, 0.01, 0.005, 0.001, and 0.0001, were analyzed, respectively. Images and total number of false-positive voxels at each *P*-value threshold were generated and computed.

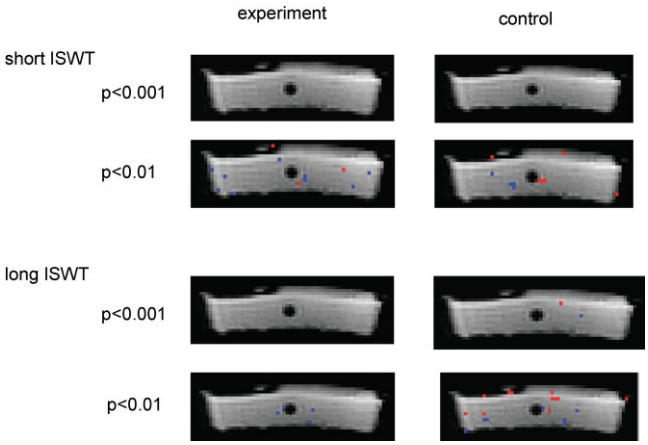

Figure 2. Images of false-positive reaction for experimental and control conditions with both short and long ISWT. Two *P*-value thresholds, $P < 0.001$ and $P < 0.01$, are shown here. Voxels with false-positive activation are denoted in red, and voxels with false-positive deactivation are denoted in blue. The hypointensity area located at the center of the phantom is due to susceptibility artifact arising from the DBS electrodes.

RESULTS

Figure 2 shows images of false-positive reactions for both experimental and control conditions at $P < 0.001$ and $P < 0.01$, and both with short and long ISWT. Voxels with significant activation are denoted in red, and voxels with significant deactivation were denoted in blue. The hypointensity area located at the center of the phantom was due to susceptibility artifact arising from the DBS electrodes. We did not observe any apparent RF artifacts in the raw EPI images, which demonstrated acceptable electrical isolation along the connecting cable (5,14). The image patterns of false-positive activation/deactivation are very similar between experimental and control conditions across *P*-value levels and ISWT intervals. As expected, the number of pixels showing false-positive reaction increases as the *P*-value threshold increases. For *P*-value threshold at 0.001 and 0.0001, the false-positive images show limited or no activation/deactivation.

The total number of voxels of false-positive activation/deactivation is shown in Fig. 3. For all conditions, numbers of false-positive activated/deactivated voxels increase with increasing *P*-value, and are near zero at $P < 0.001$ and $P < 0.0001$. In Fig. 3a, the control condition (dashed lines) seems to have slightly more false-positive activation voxels than the experimental condition. However, this was not observed in the results of false-positive deactivation (Fig. 3b), and was without statistical significance. Otherwise, all curves show no significant differences between conditions (experimental and control) and lengths of ISWT.

DISSCUSSION

During the past decade, DBS has become an established treatment for patients suffering from medically intractable chronic pain, Parkinson's disease, or seizures. Despite its effectiveness, the underlying mechanisms of DBS are still not clear. Researchers have tried to use imaging techniques to evaluate the efficiency of DBS and fMRI as an effective and noninvasive tool to elucidate the relevant neuronal circuitry and mechanisms underlying DBS.

A few previous studies have tried to explore and localize related neuronal pathways during DBS using fMRI on patients with implanted thalamic and subthalamic electrodes (2–4). Also, two studies proposed safety recommendations for combining DBS treatment with fMRI examination (1,5). However, there were no reports on validating results of fMRI associated with DBS and no studies on imaging experiment paradigms. In this gel-filled phantom study, we analyzed the volumes of false-positive activation and deactivation in experimental/control conditions with short/long ISWT. The results demonstrated that the numbers of false-positive activation/deactivation voxels appear not significantly different between conditions and ISWT. However, the false-positive activation/deactivation volumes did increase with decreasing *P*-value threshold. From this experiment, the false-positive reactions were negligible at $P < 0.001$ and $P < 0.0001$.

In conclusion, our findings indicated that false-positive findings from fMRI data processing of similar object size in DBS experiments can be well controlled with a statistical threshold of $P < 0.001$ or tighter. With two-second stimulation, the short ISWT of 3500 msec did not increase false-positive reactions compared to the long ISWT of 5160 msec. These results may help future paradigm design for fMRI experiments during DBS.

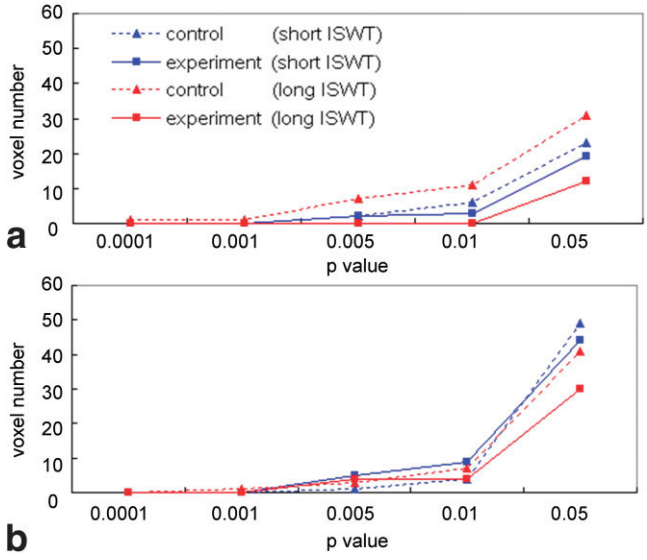

Figure 3. The number of voxels with false-positive reaction vs. different *P*-value thresholds from 0.0001 to 0.05. **a:** Voxels with false-positive activation. **b:** Voxels with false-positive deactivation. The experimental conditions are denoted as solid lines whereas the control conditions are dashed lines. Blue lines represent results of short ISWT, and red lines are for long ISWT.

REFERENCES

1. Weaver F, Follett K, Hur Kwan, Ippolito D, Stern M. Deep brain stimulation in Parkinson disease: a meta-analysis of patient outcomes. J Neurosurg 2005;103:956–967.
2. Kerrigan JF, Litt B, Fisher RS, et al. Electrical stimulation of the anterior nucleus of the thalamus for the treatment of intractable epilepsy. Epilepsia 2004;45:346–354.
3. Stefurak T, Mikulis D, Mayberg H, et al. Deep brain stimulation for Parkinson's disease dissociates mood and motor circuits: a functional MRI case study. Mov Disord 2003;18:1508–1516.
4. Bejjani B-P, Damier P, Arnulf I, et al. Transient acute depression induced by high-frequency deep-brain stimulation. N Engl J Med 1999;340:1476–1480.
5. Georgi JG, Stippich C, Tronnier VM, Heiland S. Active deep brain stimulation during MRI: a feasibility study. Magn Reson Med 2004; 51:380–388.
6. Jech R, Urgosik D, Tintera J, et al. Functional magnetic resonance imaging during deep brain stimulation: a pilot study in four patients with Parkinson's disease. Mov Disord 2001;16: 1126–1132.
7. Rezai AR, Lozano AM, Crawley AP, et al. Thalamic stimulation and functional magnetic resonance imaging: localization of cortical and subcortical activation with implanted electrodes. J Neurosurg 1999;90:583–590.
8. Hsu YY, Liu HL, Wu T, Lee ST. Blood oxygenation level-dependent functional MRI during deep brain stimulation to anterior thalamic nucleus in a seizure patient. In: Proceedings of the 11th Annual Meeting of ISMRM, Toronto, Ontario, Canada, 2003 (Abstract 2500).
9. Kato H, Hiraoka M, Ishida T. An agar phantom for hyperthermia. Med Phys 1986;13:396–398.
10. Shapiro EM, Borthakur A, Reddy R. MR imaging of RF heating using a paramagnetic doped agarose phantom. MAGMA 2000;10: 114–121.
11. Geddes LA, Baker LE. The specific resistance of biological material —a compendium of data for the biomedical engineer and physiologist. Med Biol Eng 1967;5:271–293
12. Malmivuo J, Plonsey R. Bioelectromagnetism: principles and applications of bioelectric and biomagnetic fields. New York: Oxford University Press; 1995;455–461.
13. Theodore WH, Fisher RS. Brain stimulation for epilepsy. Lancet Neurol 2004;3:111–118.
14. Arantes PR, Cardoso EF, Barreiros MA, et al. Performing functional magnetic resonance imaging in patients with Parkinson's disease treated with deep brain stimulation. Mov Disord 2006;21:1154–1162.